Chapter 1

COOPERATIVE CONTROL OF ROBOT FORMATIONS

Rafael Fierro, Peng Song, Aveek Das, and Vijay Kumar

GRASP Lab. University of Pennsylvania, Philadelphia PA, USA

rfierro, pengs, aveek, kumar@grasp.cis.upenn.edu

Abstract   We describe a framework for controlling and coordinating a group of nonholonomic mobile robots equipped with range sensors, with applications ranging from scouting and reconnaissance, to search and rescue and manipulation tasks. We derive control algorithms that allow the robots to control their position and orientation with respect to neighboring robots or obstacles in the environment. We then outline a coordination protocol that automatically switches between the control laws to maintain a specified formation. Two simple trajectory generators are derived from potential field theory. The first allows each robot to plan its reference trajectory based on the information available to it. The second scheme requires sharing of information and enables a rigid group formation. Numerical simulations illustrate the application of these ideas and demonstrate the scalability of the proposed framework for a large group of robots.

Keywords: Formation control, potential functions, nonholonomic mobile robots, switching control.

1.   Introduction

It is well known that there are several tasks that can be performed more efficiently and robustly using multiple robots, see for example (Parker, 2000). Multi-robot applications include cooperative manipulation, navigation and planning, collaborative mapping and exploration, and formation control. In fact, there is extensive literature on motion planning and control of mobile robots in structured environments. However, traditional control theory mostly enables the design of controllers in a single mode of operation, in which the task and the model of the

system are fixed. While control and estimation theory allows us to model each behavior as a dynamical system, it does not give us the tools to compose behaviors or the hierarchy that might be inherent in the switching behavior, or to predict the global performance of a highly complex multi–robotic system.

The key contributions of this paper are (1) a set of control algorithms and a coordination strategy that allow the robots to maintain a prescribed formation, and (2) a newly developed trajectory generator that combines potential functions and the dynamics of visco-elastic contacts. By combining control, coordination, and trajectory generation we are able to compose single control modes or behaviors and build formations in a modular fashion. Moreover, we can guarantee that under reasonable assumptions the basic formation is stable. Thus, the group can maintain a desired formation and flow towards its goal configuration. The ability to maintain a prescribed formation allows the robots to perform a variety of tasks such as collaborative mapping and exploration, and cooperative manipulation (Spletzer et al., 2001).

We divide the multi-robot cooperative control problem into two areas: (a) *formation control* and (b) *trajectory generation*. Formation control approaches can be classified into three main categories as in (Beard et al., 1999): *leader-following*, *behavioral* and *virtual structures*. In the leader-following one robot acts as a leader and generates the reference trajectory for the team of robots. Thus, the behavior of the group is defined by the behavior of the leader. In the behavioral approach, a number of basic behaviors is prescribed, *e.g.*, obstacle avoidance, formation keeping, and goal seeking. The overall control action (*emergent behavior*) is a weighted average of the control actions for each basic behavior. In this case, composing control strategies for competing behaviors and implementing them can be straightforward. However, formal stability analysis of the emergent group behavior may be difficult. Finally, virtual structures consider the entire formation as a rigid body. Once the desired dynamics of the virtual structure are defined, then the desired motion for each agent is derived. The framework proposed in this work is flexible enough to accommodate any of these formation control approaches. It is the designer's decision to use decentralized reactive behaviors with no leader involved, leader-following, or rigid body motion to perform a given task. We will demonstrate this through numerical simulation experiments.

The problem of multi–robot trajectory generation is to generate collision free trajectories for mobile robots to reach their desired destinations. Previous approaches in this area can be broadly divided into two classes including graph based planners (Barraquand and Latombe, 1993), and potential field methods (Khatib, 1986; Koditschek, 1987). In this work

we consider the latter. Artificial potential field approaches are based on constructing repulsive potential functions around obstacles and attracting potential functions around the goal location. The design of a potential field with a global minimum at the goal configuration turns out to be difficult. Various techniques have been developed to overcome these difficulties, see for instance (Volpe and Khosla, 1990; Bemporad et al., 1996; Barraquand et al., 1992). In contrast, we propose the use of simple goal-directed fields that are not specifically designed to avoid obstacles or neighboring robotsas in (Rimon and Koditschek, 1992). Instead, when a robot is close to an obstacle, it adopts a behavior that simulates the dynamics of a visco-elastic collision guaranteeing that the actual collision never occurs. This approach can be potentially scaled to multiple (tens and hundreds) robots and to higher speeds of operation.

The rest of the paper is organized as follows. In section 2 we describe a framework that allows to hierarchically compose *planning* and *control* in a distributed fashion. Section 3 presents the suite of control algorithms and the coordination strategy for switching between these controllers. Then, we formulate the *trajectory generator* in section 4. Section 5 gives simulation results and illustrates the benefits and the limitations of this methodology underlying the implementation of cooperative control of robot formations. Finally, some concluding remarks and future work ideas are given in section 6.

2.   Framework for Cooperative Control

We describe a framework for decentralized cooperative control of multi-robotic systems that emphasizes simplicity in planning, coordination, and control. The framework incorporates a two-level control hierarchy for each robot consisting of a trajectory generation level and a coordination level as illustrated in Figure 1.1. The trajectory generator derives the reference trajectory for the robot while the coordination level selects the appropriate controller (*behavior*) for the robot.

The availability and sharing of information between the robots greatly influences the design of each level. This is particularly true at the trajectory generation level. The trajectory generator can be completely decentralized so that each robot generates its own reference trajectory based on the information available to it, through its sensors and through the communication network. Alternatively, a designated leader plans its trajectory and the other group members are able to organize themselves to following the leader. The trajectory generators are derived from potential field theory. At the coordination level we assume range sensors that allow the estimation of position of neighboring robots and obsta-
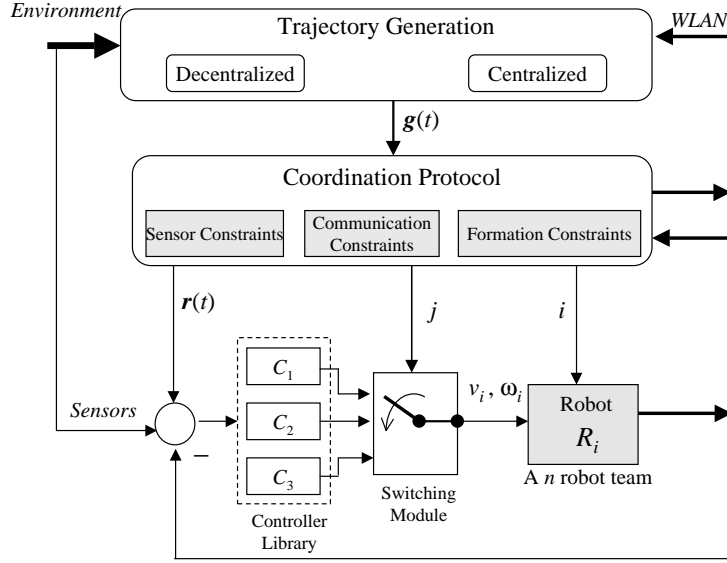
Figure 1.1.   A formation control framework.

cles. This model is motivated by our experimental platform consisting of mobile robots equipped with omni–directional cameras described in (Das et al., 2001; Alur et al., 2000). Each robot chooses from a finite set of control laws that describe its interactions with respect its neighbors (robots and obstacles) and allow it to go to a desired goal position. Thus the overall goal of this level is to prescribe the rules of mode switching and thus the dynamics of the switched system (Liberzon and Morse, 1999).

3. Formation Control

In this section, we consider a group of n nonholonomic mobile robots and describe the controllers that specify the interactions between each robot and its neighbor. The robots are velocity controlled platforms and have two independent inputs v_i and ω_i. The control laws are based on I/O feedback linearization. This means we are able to regulate two outputs. Moreover, we assume that the robots are assigned labels from 1 through n which restrict the choice of control laws. Robot 1 is the leader of the group.

We adopt a simple kinematic model for the nonholonomic robots. The kinematics of the *ith* robot are given by

$$\dot{x}_i = v_i \cos \theta_i, \quad \dot{y}_i = v_i \sin \theta_i, \quad \dot{\theta} = \omega_i \tag{1}$$

where $\boldsymbol{x}_i \equiv (x_i, y_i, \theta_i) \in SE(2)$.

In Figure 1.2, we show subgroups of two and three robots. Robot j is designated as a follower of Robot i. We first describe two controllers, adopted from (Desai et al., 1998), and derive a third controller that takes into account possible interactions with an obstacle.
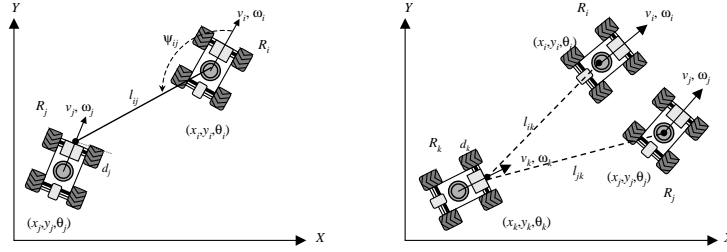

Figure 1.2. The *Separation Bearing* and *Separation Separation* Controllers.

Separation–Bearing Control. By using this controller (denoted $SB_{ij}C$ here), robot R_j follows R_i with a desired separation l_{ij}^d and desired relative bearing ψ_{ij}^d, see Figure 1.2(left). The control velocities for the *follower* are given by

$$v_j = s_{ij}\cos\gamma_{ij} - l_{ij}\sin\gamma_{ij}(b_{ij} + \omega_i) + v_i\cos(\theta_i - \theta_j) \tag{2}$$

$$\omega_j = \frac{1}{d}[s_{ij}\sin\gamma_{ij} + l_{ij}\cos\gamma_{ij}(b_{ij} + \omega_i) + v_i\sin(\theta_i - \theta_j)] \tag{3}$$

where d is the distance from the wheel axis to a reference point on the robot, and

$$\gamma_{ij} = \theta_i + \psi_{ij} - \theta j, \tag{4}$$

$$s_{ij} = k_1(l_{ij}^d - l_{ij}), \tag{5}$$

$$b_{ij} = k_2(\psi_{ij}^d - \psi_{ij}), \quad k_1, k_2 > 0 \tag{6}$$

The closed-loop linearized system is

$$\dot{l}_{ij} = k_1(l_{ij}^d - l_{ij}), \quad \dot{\psi}_{ij} = k_2(\psi_{ij}^d - \psi_{ij}), \quad \dot{\theta}_j = \omega_j \tag{7}$$

Separation–Separation Control. By using this controller (denoted $S_{ik}S_{jk}C$), robot R_k follows R_i and R_j with a desired separations l_{ik}^d and l_{jk}^d, respectively, see Figure 1.2(right). In this case the control velocities for the follower robot become

$$v_k = \frac{s_{ik}\sin\gamma_{jk} - s_{jk}\sin\gamma_{ik} + v_i\cos\psi_{ik}\sin\gamma_{jk} - v_j\cos\psi_{jk}\sin\gamma_{ik}}{\sin(\gamma_{jk} - \gamma_{ik})} \tag{8}$$

$$\omega_k = \frac{-s_{ik}\cos\gamma_{jk} + s_{jk}\cos\gamma_{ik} - v_i\cos\psi_{ik}\cos\gamma_{jk} + v_j\cos\psi_{jk}\cos\gamma_{ik}}{d\sin(\gamma_{jk} - \gamma_{ik})}$$

(9)

The closed-loop linearized system is

$$\dot{l}_{ik} = k_1(l_{ik}^d - l_{ik}), \quad \dot{l}_{jk} = k_1(l_{jk}^d - l_{jk}), \quad \dot{\theta}_k = \omega_k. \qquad (10)$$

Separation Distance–To–Obstacle Control. This controller (denoted SD_oC) allows to avoid obstacles while following a leader. Thus, the outputs of interest are the separation l_{ij} between the follower and the leader, and the distance δ from an obstacle to the follower. We define a *virtual* robot R_o as shown in Figure 1.3, which moves on the obstacle's boundary with linear velocity v_o and orientation θ_o. For this case the
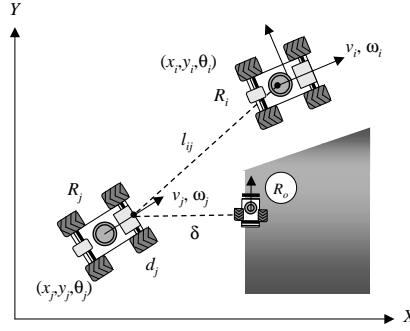

Figure 1.3. The Separation Distance to Obstacle Control *SDoC*.

velocity inputs for the follower robot R_j are given by

$$v_j = \frac{s_{ij}\cos\gamma_{oj} + s_{oj}\sin\gamma_{ij} + v_i\cos\psi_{ij}\cos\gamma_{oj}}{\cos(\gamma_{oj} - \gamma_{ij})} \qquad (11)$$

$$\omega_j = \frac{s_{ij}\sin\gamma_{oj} - s_{oj}\cos\gamma_{ij} + v_i\cos\psi_{ij}\sin\gamma_{oj}}{d\cos(\gamma_{oj} - \gamma_{ij})} \qquad (12)$$

Thus, the linearized kinematics become

$$\dot{l}_{ij} = k_1(l_{ij}^d - l_{ij}), \quad \dot{\delta} = k_o(\delta_o - \delta), \quad \dot{\theta}_j = \omega_j. \qquad (13)$$

where $s_{oj} \equiv k_o(\delta_o - \delta)$, δ_o is the desired distance from the robot R_j to an obstacle, and k_i's are positive controller gains.

It is worth noting that feedback I/O linearization is possible as long as $d\cos(\gamma_{oj} - \gamma_{ij}) \neq 0$, *i.e.*, the controller is not defined if $\gamma_{oj} - \gamma_{ij} = \pm k\frac{\pi}{2}$. This occurs when vectors $\vec{\delta}$ and $\vec{l}_{ij}$ are collinear.

By using this controller a follower robot will avoid the nearest obstacle within its *field-of-view* while keeping a desired distance from the leader. This is a reasonable assumption for many outdoor environments of practical interest. Complex environments (*e.g.*, star-like obstacles) are beyond the scope of this paper.

3.1.   A Basic Formation Building Block

In this section we develop a general approach to build formations in a modular fashion. To be more specific, since each robot in the team is nonholonomic, it is able to control up two output variables (De Luca et al., 1998), *i.e.*, a robot can follow another robot maintaining a desired separation and bearing, or follow two robots maintaining desired separations. Thus, a basic formation building block consists of a *lead* robot R_i, a *first follower* robot R_j, and a *follower* robot R_k. Figure 1.4 illustrates the basic formation and the actual robots we use in our experimental testbed. The basic idea is that R_i follows a given trajectory $g(t) \in SE(2)$, R_j and R_k use *SBC* and *SSC*, respectively.
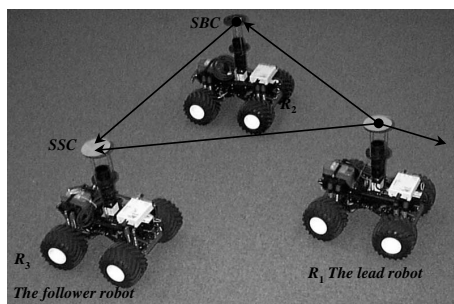

Figure 1.4.   The basic formation configuration.

3.2.   Stability Analysis

In the following, we prove that the *basic formation* is stable, that is, relative distances and bearings reach their desired values asymptotically, and the internal dynamics of R_j and R_k are stable. Since we are using I/O feedback linearization (Isidori, 1995), the linearized systems are given by (7) and (10) with outputs

$$\boldsymbol{z}_1 = [l_{ij} \quad \psi_{ij}]^T, \qquad \boldsymbol{z}_2 = [l_{ik} \quad l_{jk}]^T$$

It is straightforward to show that the output vectors $\boldsymbol{z}_{1,2}$ will converge to the desired values arbitrarily fast. However, a complete stability analysis requires the study of the internal dynamics of the robots *i.e.*, the heading

angles θ_j and θ_k which depend on the controlled angular velocities ω_j and ω_k.

Theorem 1 *Assume that the lead vehicle's linear velocity along the path $g(t) \in SE(2)$ is lower bounded i.e., $v_i \geq V_{\min} > 0$, its angular velocity is also bounded i.e., $\|\omega_i\| < W_{\max}$, the relative velocity $\delta_v \equiv v_i - v_j$ and relative orientation $\delta_\theta \equiv \theta_i - \theta_j$ are bounded by small positive numbers ε_1, ε_2, and the initial relative orientations $\|\theta_i(t_0) - \theta_j(t_0)\| < c_1\pi$, $\|\theta_i(t_0) - \theta_k(t_0)\| < c_2\pi$ with $0 < c_{1,2} < 1$. If the control velocities (2)–(3) are applied to R_j, and the control velocities (8)–(9) are applied to R_k, then the formation is stable, and the system outputs l_{ij}, ψ_{ij}, l_{ik}, and l_{jk} converge exponentially to the desired values.*

Proof: Let the system error $\boldsymbol{e} = [e_1 \cdots e_6]^T$ be defined as

$$
\begin{aligned}
e_1 &= l_{ij}^d - l_{ij}, \quad e_2 = \psi_{ij}^d - \psi_{ij}, \quad e_3 = \theta_i - \theta_j \\
e_4 &= l_{ik}^d - l_{ik}, \quad e_5 = l_{jk}^d - l_{jk}, \quad e_6 = \theta_i - \theta_k
\end{aligned}
\tag{14}
$$

We need to show that the internal dynamics of R_j and R_k are stable which in formation control, is equivalent to show that the orientation errors e_3, e_6 are bounded. For the first follower R_j, we have

$$
\dot{e}_3 = \omega_i - \omega_j
$$

after some algebraic simplification, we obtain

$$
\dot{e}_3 = -\frac{v_i}{d} \sin e_3 + \eta_1(e_3, \omega_i, e_1, e_2)
\tag{15}
$$

where

$$
\eta_1(t, e_3) = (1 - \frac{l_{ij}}{d} \cos \gamma_{ij}) \omega_i - \frac{1}{d}(k_1 e_1 \sin \gamma_{ij} + k_2 e_2 l_{ij} \cos \gamma_{ij})
$$

The nominal system *i.e.*, $\eta_1(t, e_3) = 0$ is given by

$$
\dot{e}_3 = -\frac{v_i}{d} \sin e_3
\tag{16}
$$

which is (locally) exponentially stable provided that the velocity of the lead robot $v_i > 0$. Since ω_i is bounded, it can be shown that $\|\eta_1(t, e_3)\| \leq \delta_1$. By using stability theory of perturbed systems (Khalil, 1996), and the condition of the theorem $\|e_3(t_0)\| < c_1\pi$ for some positive constant $c_1 < 1$, then

$$
\|e_3(t)\| \leq \sigma_1, \qquad \forall\, t \geq t_1
$$

for some finite time t_1. Now for the follower R_k, the error system becomes

$$
\dot{e}_6 = \omega_i - \omega_k
$$

as before and after some work, we obtain

$$\dot{e}_6 = -\frac{v_i}{d}\sin e_6 + \eta_2(e_6, \omega_i, e_4, e_5, \delta_v, \delta_\theta) \tag{17}$$

where

$$\eta_2(t, e_6) = \omega_i - \frac{v_i \delta_\theta \sin \psi_{jk} \cos(e_6 - \psi_{jk}) + \delta_v \cos(e_6 + \psi_{ik}) \cos \psi_{jk}}{d[\delta_\theta \cos(\psi_{jk} - \psi_{ij}) + \sin(\psi_{jk} - \psi_{ij})]} -$$
$$- \frac{k_5 e_5 \cos \gamma_{ij} + k_4 e_4 \cos \gamma_{jk}}{d[\delta_\theta \cos(\psi_{jk} - \psi_{ij}) + \sin(\psi_{jk} - \psi_{ij})]}$$

Again, the nominal system is given by (16) *i.e.*, $\eta_2(t, e_6) = 0$, and it is (locally) exponentially stable provided that the velocity of the lead robot $v_i > 0$. Since $\|\omega_i\| < W_{\max}$, $\|\delta_v\| < \varepsilon_1$, and $\|\delta_\theta\| < \varepsilon_2$, it can be shown that $\|\eta_2(t, e_6)\| \le \delta_2$. Knowing that $\|e_6(t_0)\| < c_2 \pi$ for some positive constant $c_2 < 1$, then

$$\|e_6(t)\| \le \sigma_2, \qquad \forall \, t \ge t_2$$

for some finite time t_2.

$\square$

The above theorem shows that, under some reasonable assumptions, the three-robot formation system is stable *i.e.*, there exists a Lyapunov function $V(t, e)$ in $[0, \infty) \times D$, where $D = \{e \in \Re^6 | \, \|e\| < c\}$, such that $\dot{V}(t, e) \le 0$. Let

$$V = e_{12}^T \boldsymbol{P}_{12} e_{12} + \frac{1}{2} e_3^2 + e_{45}^T \boldsymbol{P}_{45} e_{45} + \frac{1}{2} e_6^2 \tag{18}$$

be a Lyapunov function for the system error (14) then

$$\dot{V} = -e_{12}^T \boldsymbol{Q}_{12} e_{12} - e_{45}^T \boldsymbol{Q}_{45} e_{45} - \frac{v_i}{d} e_3 \sin e_3 \tag{19}$$
$$- \frac{v_i}{d} e_6 \sin e_6 + \eta_1(t, e_3) e_3 + \eta_2(t, e_6) e_6$$

where $e_{12}^T \equiv [e_1 \quad e_2]$, $e_{45}^T \equiv [e_4 \quad e_5]$, and $\boldsymbol{P}_{12}$, $\boldsymbol{P}_{45}$, $\boldsymbol{Q}_{12}$, and $\boldsymbol{Q}_{45}$ are 2×2 positive definite matrices. By looking at (18)-(19), we can study some particular formations of practical interest.

- Let us assume two robots in a *linear motion* leader-following formation *i.e.*, v_i is constant, and $\omega_i = 0$. Thus the Lyapunov function and its derivative become

$$V_2 = e_{12}^T \boldsymbol{P}_{12} e_{12} + \frac{1}{2} e_3^2 \tag{20}$$

$$\dot{V}_2 = -\boldsymbol{e}_{12}^T \boldsymbol{Q}_{12} \boldsymbol{e}_{12} - \frac{v_i}{d} e_3 \sin e_3 \qquad (21)$$

then the two-robot system is (locally) asymptotically stable *i.e.*, $e_3 \to 0$ as $t \to \infty$ provided that $v_i > 0$ and $\|e_3\| < \pi$. If ω_i is constant (circular motion), then e_3 is bounded. It is well-known that an optimal nonholonomic path can be planned by joining linear and circular trajectory segments. This result can be extended to n robots in a *convoy-like* formation (*c.f.*, (Canudas-de-Wit and NDoudi-Likoho, 2000). Let us consider a team of n robots where R_i follows R_{i-1} under *SBC*. A Lyapunov function and its derivative can be given by

$$V_{1...n} = \sum_{i=2}^{n} \boldsymbol{e}_{i-1,i}^T \boldsymbol{P}_{i-1,i} \boldsymbol{e}_{i-1,i} + \frac{1}{2} e_{\theta i}^2 \qquad (22)$$

$$\dot{V}_{1...n} = -\sum_{i=2}^{n} (\boldsymbol{e}_{i-1,i}^T \boldsymbol{Q}_{i-1,i} \boldsymbol{e}_{i-1,i} + \frac{v_i}{d} e_{\theta i} \sin e_{\theta i} - \eta_i(t, e_{\theta i})) \qquad (23)$$

where $\boldsymbol{e}_{i-1,i} = [l_{i-1,i}^d - l_{i-1,i} \quad \pi - \psi_{i-1,i}]^T$ is the output error, and $e_{\theta i} = \theta_{i-1} - \theta_i$ is the orientation error between R_{i-1} and R_i.

- A similar analysis can be carried out for the case of three robots in a *parallel* linear motion where $v_i = v_j = constant$, $\omega_i = \omega_j = 0$, and $\theta_i(t_0) = \theta_j(t_0)$. The Lyapunov function and its derivative are given by

$$V_3 = \boldsymbol{e}_{45}^T \boldsymbol{P}_{45} \boldsymbol{e}_{45} + \frac{1}{2} e_6^2 \qquad (24)$$

$$\dot{V}_3 = -\boldsymbol{e}_{45}^T \boldsymbol{Q}_{45} \boldsymbol{e}_{45} - \frac{v_i}{d} e_6 \sin e_6 \qquad (25)$$

then the three-robot system is (locally) asymptotically stable *i.e.*, $e_6 \to 0$ as $t \to \infty$ provided that $v_i > 0$, $\|e_6\| < \pi$ and $l_{ij} < l_{ik} + l_{jk}$. Again, this result can be extended to n robots in parallel linear formation.

3.3.   Coordination Strategy

So far, we have shown that under certain assumptions a group of robots can navigate maintaining a stable formation. However, in real situations mobile robotic systems are subject to sensor, actuator and communication constraints, and have to operate within unstructured environments. These problems have motivated the development of a *switching paradigm* that allows robots change the shape of the formation *on-the-fly*. The basic strategy is as follows. Suppose a two-robot (R_1,

R_2) formation is following a predefined trajectory using *SBC*. If there is an obstacle in the field-of-view of the follower, it switches to *SDoC*. When the obstacle has been successfully negotiated, R_2 switches back to *SBC*. Assume now a third robot R_3 joins the formation. Since R_3 has some sensor constraints, it may *see* or *follow* R_1, R_2 or both. For avoiding inter-robot collisions, the preferred configuration is that R_3 follows R_1 and R_2 using *SSC*. Thus, if R_3 sees only R_2, it will follow R_2 with desired values (*i.e.* l_{23}^d, ψ_{23}^d) selected in a way that R_3 is driven to the domain of controller *SSC*. Similarly, if R_3 sees only R_1, the desired output values (l_{13}^d, ψ_{13}^d) are chosen such that R_3 is driven to the domain of controller *SSC*. Furthermore, assume R_4 joints the group. It has six control possibilities to choose from as follows. R_4 may follow R_1, R_2, R_3, or any pair $R_1 R_2$, $R_1 R_3$, $R_2 R_3$. The preferred configuration and desired values will depend on the prescribed formation shape and size.

This algorithm can be recursively extended to n robots. Let us consider a 4–robot case shown in Figure 1.5. To define a formation, we need
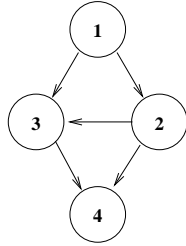

Figure 1.5. Control graph for 4 robots.

one separation–bearing control (R_2 following R_1) and two separation–separation controllers (R_3 following R_1 and R_2, and R_4 following R_2 and R_3). We call such a directed graph $\mathcal{H}$, a *control graph*. In a control graph, nodes and edges represent robots and control policies, respectively. Any control graph can be described by its *adjacency matrix* ((Nemhauser and Wolsely, 1988)). For this example, the adjacency matrix becomes

$$H = \begin{bmatrix} 0 & 1 & 1 & 0 \\ 0 & 0 & 1 & 1 \\ 0 & 0 & 0 & 1 \\ 0 & 0 & 0 & 0 \end{bmatrix} \tag{26}$$

Note that this is a directed graph with the control flow from leader i to follower j. If a column k has a non zero entry in row i, then robot k is following i. A robot can have up to 2 leaders. The column with all zeros corresponds to the *lead* robot. A row with all zeros corresponds to a *terminal* follower.

It is clear that the number of possible control graphs increases dramatically with the number of robots. For labeled robots with the constraint of leaders having lower labels than followers, $n = 3$ allows 3 control graphs, $n = 4$ results in 18 graphs, and $n = 5$ results in 180 graphs.

The coordination strategy allows decentralized decision making for each individual robot. This is especially useful in simulations of large formations in complex scenarios to keep track of individual choice of controllers and switching between them. A formal study of control graphs in the context of formation control is a topic of current and future work (Fierro et al., 2001).

4.   Trajectory Generation Using Contact Dynamics Models

In this section, we propose a scheme for sensor-based trajectory generation. The key idea that distinguishes our approach from previous work is the use of rigid body contact dynamics models to allow collisions between the robot and its surroundings instead of avoiding them.

Consider a group of mobile robots moving in an environment with the presence of obstacles, we first characterize the surrounding spatial division of each mobile robot with three zones as depicted in Figure 1.6. Use robot R_1 as an example, the *sensing zone* denotes the region within which a robot can detect obstacles and other robots. The *contact zone* is a collision warning zone. The robot starts estimating the relative positions and velocities of any objects that may appear inside its contact zone. The innermost circle is the *protected zone* which is modeled as a rigid core during a possible contact. The *ellipse* within the protected zone represents the *reachable* region of the robot. It is pre-computed based on the robot's maximum kinetic energy. Thus, the actual robot is protected from collisions. In the planning process, we will use the protected zone as an abstraction of the robot itself.

The dynamics equations of motion for the ith nonholonomic robot in the group are given by

$$M_i(q_i)\ddot{q}_i + h_i(q_i, \dot{q}_i) = B_i(q_i)u_i - A_i(q_i)^T\lambda_i + \sum_{j=1}^{k} W_{ij}F_{ij} \quad (27)$$

$$A_i(q_i)\dot{q}_i = 0 \quad (28)$$

where $q_i \in \Re^3$ is the vector of generalized coordinates, M_i is an 3×3 positive-definite symmetric inertia matrix, $h_i(q_i, \dot{q}_i)$ is a 3×1 vector of nonlinear inertial forces, B is a 3×2 input transformation matrix, A_i is a 3×1 matrix associated with the nonholonomic constraints, λ is the corresponding constraint force, and u_i is the 3×1 vector of applied
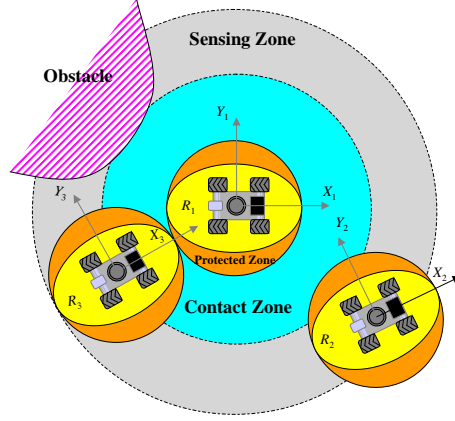
Figure 1.6. Zones for the computation of contact response.

(external) forces and torques. k is the number of the contacts between the ith–robot and all other objects which could be either obstacles or other robots. $F_{ij} = (F_{N,ij} \; F_{T,ij})^T$ is a 2×1 vector of contact forces corresponding to the jth contact, and $W_{ij} \in \Re^{3 \times 2}$ is the Jacobian matrix that relates the velocity at the jth contact point to the time derivatives of the generalized coordinates of the robot.

We adopt a state-variable based compliant contact model described in (Song et al., 2001) to compute the contact forces. At the jth contact of the agent i, the normal and tangential contact forces $F_{N,ij}$ and $F_{T,ij}$ are given by

$$F_{N,ij} \;=\; f_N(\delta_{N,ij}) + g_N(\delta_{N,ij}, \dot{\delta}_{N,ij}), \quad j=1,\ldots,k, \qquad (29)$$

$$F_{T,ij} \;=\; f_T(\delta_{T,ij}) + g_T(\delta_{T,ij}, \dot{\delta}_{T,ij}), \quad j=1,\ldots,k, \qquad (30)$$

where the functions f_N and f_T are the elastic stiffness terms and g_N and g_T are the damping terms in the normal and tangential directions respectively. Similar to handling rigid body contact, these functions can be designed to adjust the response of the robot. $\delta_{N,ij}(q)$ and $\delta_{T,ij}(q)$ are the local normal and tangential deformations which can be uniquely determined by the generalized coordinates of the system. The details and variations on the compliant contact model are discussed in (Kraus and Kumar, 1997; Song et al., 2001). A key feature of this model is that it allows to resolve the ambiguous situations when more than three objects came into contact with one robot.

Figure 1.7 shows an example of an army-ant scenario in which 25 *holonomic* robots try to arrange themselves around a goal. The grouping

14

is done dynamically using a decentralized decision making process. The team is initialized with two groups. A quadratic well type of potential function (Khatib, 1986; Koditschek, 1987) is constructed to drive the robots toward the goal. The expression of the potential function is given by

$$\phi(q) = \frac{k_p}{2}(q - q_g)^T(q - q_g) \tag{31}$$

where q_g is the coordinates of the goal. The input u_i for the ith agent can be obtained by the gradient of the potential function

$$u_i = -\nabla\phi(q_i) = -k_p(q - q_g) \tag{32}$$

which is a proportional control law. Asymptotic stabilization can be achieved by adding dissipative forces (Khatib, 1986).
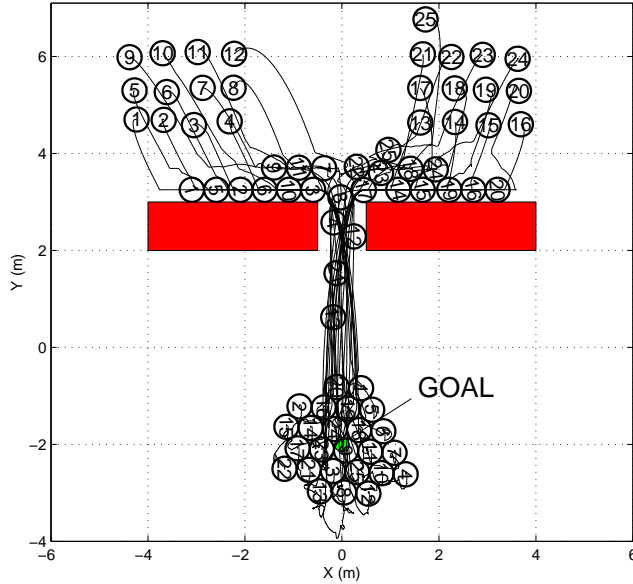

Figure 1.7. 25 holonomic robots arrange themselves around a target.

For the nonholonomic case substantial care in developing the local level controllers (Barraquand and Latombe, 1993; Bemporad et al., 1996) is required. We project the contact forces $\sum_{j=1}^{k} W_{ij}F_{ij}$ in (27) onto the reduced space while eliminating the constraint forces $A_i(q_i)^T\lambda_i$ in (28). As in (Fierro and Lewis, 1999), we use I/O linearization techniques to generate a control law u that stabilizes the robot's configuration about a reference trajectory, *i.e.*, $\|q - q_d\| \to 0$ as $t \to \infty$. The projected contact

forces are treated as external disturbances during this process. We refer the reader to (Fierro et al., 2001) for details.

This approach can be potentially scaled to tens and hundreds of robots. Each vehicle is driven by a set of local controllers that uses the information obtained within its local sensing zone. Thus, explicit inter–robot communication is avoided. We will illustrate the application of this method in the next section.

5.   Simulation Results

We illustrate our approach by an example in which 4 nonholonomic mobile robots $R_{1,2,3,4}$ are commanded to a goal position within an unknown environment. In the first experiment, the robots are autonomous, and the formation constraint is not explicitly enforced. Each robot runs its own trajectory generator and controller. As it can be seen in Figure 1.8, the robots are able to navigate and reach the goal position.
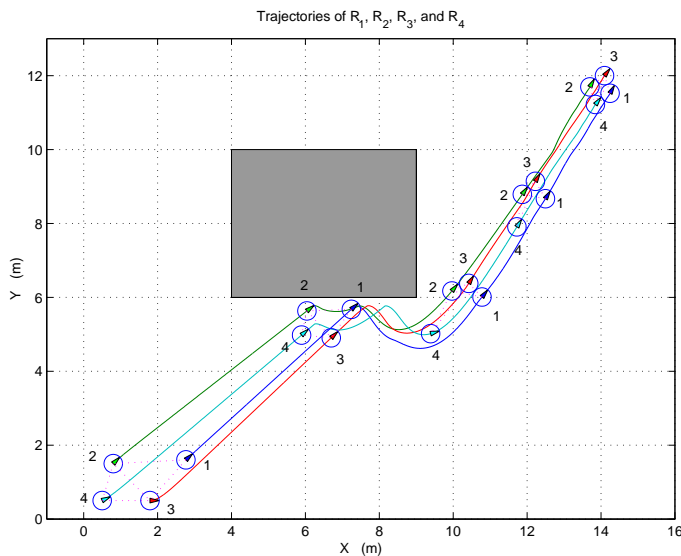

Figure 1.8.   Decentralized trajectory generation and control.

In a second experiment, the trajectory generator produces a trajectory only for the lead robot R_1. Then, the basic controllers and the coordination strategy outlined in section 3 are implemented on $R_{2,3,4}$. The desired shape of the formation is a *diamond* with inter-robot separation of 1.2 m. In order to reach the desired formation, R_2 follows R_1 with $SB_{12}C$. R_3 has to maintain a specified distance from R_1 and R_2,

i.e., $S_{13}S_{23}C$. Similarly, R_4 is to maintain a specified distance from R_2 and R_3, *i.e.*, $S_{24}S_{34}C$. However, $R_{2,3,4}$ may switch controllers depending on their relative positions and orientations with respect to neighboring robots or obstacles. Thus, for a initial formation, the group is able to reconfigure itself until the desired formation shape is achieved. Figure 1.9 shows that robots are able to negotiate the obstacle, avoid collisions and keep the formation shape.
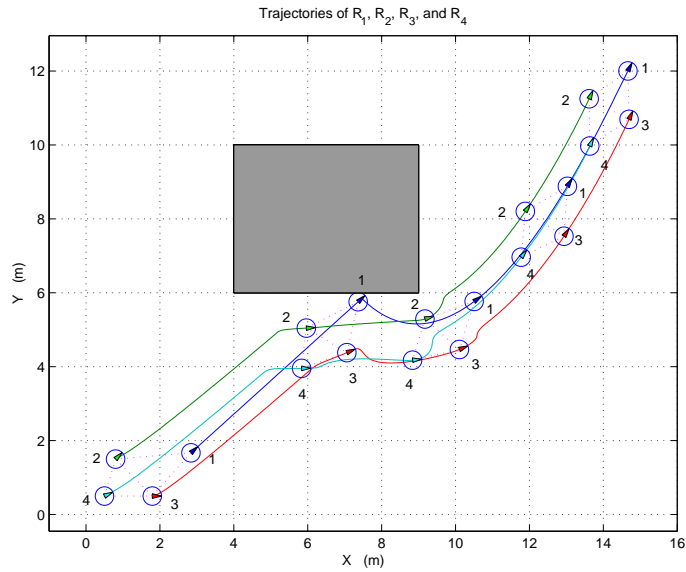

Figure 1.9.   Leader–following formation control.

Finally, we repeat the last simulation experiment, but this time the lead robot's trajectory is generated considering the mass/inertia of the entire group (*i.e.*, the group is seen as a rigid body). The behavior of the group of robots is depicted in Figure 1.10. The resulting trajectory is different than the previous case, but computationally more intensive.

These simulation exercises illustrate the flexibility of the proposed framework. We have implemented behavior–based navigation, leader-following and virtual structure formation in a straightforward manner. This flexibility will be useful in actual multi-robotic missions where autonomous vehicles may need to navigate in a decentralized fashion until a target has been detected. Then the group can switch to a leader-following behavior and keep a desired formation shape around the target. Finally, a rigid formation (desired shape and size) behavior can be switched in to manipulate and transport the target.
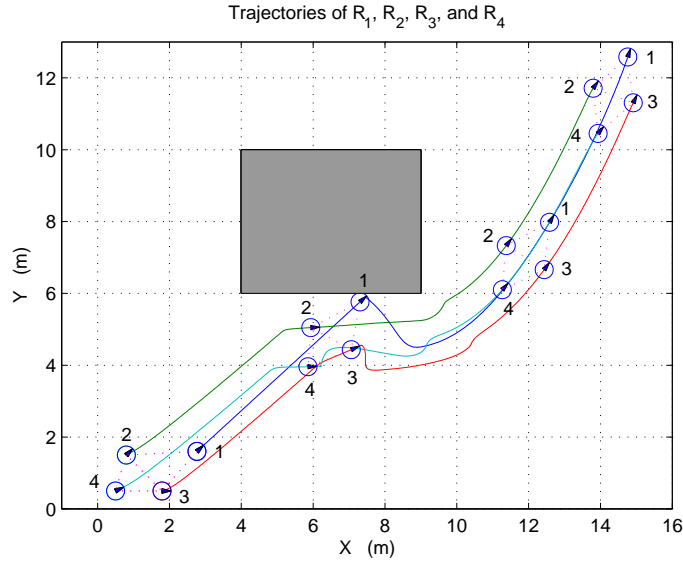
Figure 1.10. Centralized trajectory generation with decentralized control.

6.   Conclusions

In this paper, we presented a framework for controlling and coordinating a group of nonholonomic mobile robots. The framework integrates three key components for cooperative control of robot formations: (1) reference trajectory generation, (2) a coordination strategy that allows the robots to switch between control policies, and (3) a suite of controllers that under reasonable assumptions guarantees stable formations. Our approach can easily scale to any number (tens and hundreds) of vehicles and is flexible enough to support many formation shapes. The framework described here can also be applied to other types of unmanned vehicles (*e.g.*, aircraft, spacecraft, and underwater vehicles). Currently, we are formalizing and extending the coordination strategy for a large number of robots, and conducting experiments on a group of car-like mobile platforms equipped with on-board omni–directional vision system. Also, we are applying these ideas to formation flight of multiple unmanned aerial vehicles $UAVs$ on $SE(3)$.

Acknowledgments

References

Alur, R., Das, A., Esposito, J., Fierro, R., Hur, Y., Grudic, G., Kumar, V., Lee, I., Ostrowski, J. P., Pappas, G., Southall, J., Spletzer, J., and Taylor, C. J. (2000). A framework and architecture for multirobot coordination. In *Proc. ISER00, Seventh International Symposium on Experimental Robotics*, Honolulu, Hawaii.

Barraquand, J., Langlois, B., and Latombe, J. (1992). Numerical potential field techniques for robot path planning. *IEEE Trans. Syst., Man, and Cyber.*, 22(2):224–241.

Barraquand, J. and Latombe, J. (1993). Non-holonomic multibody mobile robots: controllability and motion planning in the presence of obstacles. *Algorithmica*, 10:121–155.

Beard, R. W., Lawton, J., and Hadaegh, F. Y. (1999). A coordination architecture for spacecraft formation control. Submitted to IEEE Trans. Contr. Sys. Technology.

Bemporad, A., De Luca, A., and Oriolo, G. (1996). Local incremental planning for a car-like robot navigating among obstacles. In *Proc. IEEE Int. Conf. Robot. Automat.*, pages 1205–1211.

Canudas-de-Wit, C. and NDoudi-Likoho, A. D. (2000). Nonlinear control for a convoy-like vehicle. *Automatica*, 36:457–462.

Das, A., Fierro, R., Kumar, V., Southall, J., Spletzer, J., and Taylor, C. J. (2001). Real-time vision based control of a nonholonomic mobile robot. To appear in IEEE Int. Conf. Robot. Automat., ICRA01.

De Luca, A., Oriolo, G., and Samson, C. (1998). Feedback control of a nonholonomic car-like robot. In Laumond, J.-P., editor, *Robot Motion Planning and Control*, pages 171–253. Springer-Verlag, London.

Desai, J., Ostrowski, J. P., and Kumar, V. (1998). Controlling formations of multiple mobile robots. In *Proc. IEEE Int. Conf. Robot. Automat.*, pages 2864–2869, Leuven, Belgium.

Fierro, R. and Lewis, F. L. (1999). Robot kinematics. In Webster, J., editor, *Wiley Encyclopedia of Electrical and Electronics Engineering*. John Wiley and Sons, Inc.

Fierro, R., Song, P., Das, A., and Kumar, V. (2001). A framework for scalable cooperative navigation of autonomous vehicles. Technical report MS-CIS-01-09, Department of Computer and Information Science, University of Pennsylvania, Philadelphia PA, USA.

Isidori, A. (1995). *Nonlinear Control Systems*. Springer-Verlag, London, 3rd edition.

Khalil, H. (1996). *Nonlinear Systems*. Prentice Hall, Upper Sadle River, NJ, 2nd edition.

Khatib, O. (1986). Real-time obstacle avoidance for manipulators and mobile robots. *International Journal of Robotics Research*, 5:90–98.

Koditschek, D. (1987). Exact robot navigation by means of potential functions: Some topological considerations. In *Proc. IEEE Int. Conf. Robot. Automat.*, pages 1–6.

Kraus, P. R. and Kumar, V. (1997). Compliant contact models for rigid body collisions. In *Proceedings of IEEE International Conference on Robotics and Automation*, pages 1382–1387.

Liberzon, D. and Morse, A. S. (1999). Basic problems in stability and design of switched systems. *IEEE Control Systems*, 19(5):59–70.

Nemhauser, G. L. and Wolsely, L. A. (1988). *Integer and Combinatorial Optimization*, chapter I.3. Wiley.

Parker, L. E. (2000). Current state of the art in distributed autonomous mobile robotics. In Parker, L. E., Bekey, G., and Barhen, J., editors, *Distributed Autonomous Robotic Systems*, volume 4, pages 3–12. Springer, Tokio.

Rimon, E. and Koditschek, D. (1992). Exact robot navigation using artificial potential fields. *IEEE Trans. Robot. & Autom.*, 8(5):501–518.

Song, P., Kraus, P., Kumar, V., and Dupont, P. (2001). Analysis of rigid–body dynamic models for simulation of systems with frictional contacts. *Tran. ASME*, 68:118–128.

Spletzer, J., Das, A., Fierro, R., Taylor, C. J., Kumar, V., and Ostrowski, J. P. (2001). Cooperative localization and control for multi-robot manipulation. Submitted to IEEE/RSJ Int. Conf. Intell. Robots and Syst., IROS2001.

Volpe, R. and Khosla, P. (1990). Manipulator control with superquadric artificial potential functions: Theory and experiments. *IEEE Trans. on Syst., Man, and Cyber.*, 20(6):1423–1436.